REFERENCES

[1] D. V. Otto, "The admittance of cylindrical antennas driven from a coaxial-line," *Radio Sci.*, vol. 2, pp. 1031–1042, 1967.
[2] A. G. Williamson, "Analysis and modelling of a coaxial-line/rectangular waveguide junction," *IEEE Proc. H, Microwaves, Opt. Antennas*, vol. 129, no. 5, pp. 262–270, 1982.
[3] ——, "Radial-line/coaxial-line junctions: analysis and equivalent circuits," *Int. J Electronics*, vol. 5, no. 1, pp. 91–104, 1985.
[4] M. E. Bialkowski, "Analysis of a coaxial-to-waveguide adaptor incorporating a dielectric coated probe." *Microwave Guided Wave Lett.*, vol. 1, no. 8, pp. 211–214.
[5] G. N. Watson, *A Treatise on the Theory of Bessel Functions*. London: Cambridge University Press, 1966.

A Rigorous Analysis of a Shielded Microstrip Asymmetric Step Discontinuity

C. N. Capsalis, N. K. Uzunoglu, C. P. Chronopoulos, and Y. D. Sigourou

***Abstract*—In this paper microstrip asymmetric step discontinuities are analyzed using a mode-matching technique leading to the frequency-dependent characteristics of the structure. On both sides of the discontinuity the fields are expanded in terms of the normal even and odd hybrid modes of shielded microstrip lines, taking into account not only the propagating modes but also higher order even and odd modes, which are evanescent-type waves. The propagation constants of the even and odd hybrid modes are computed using a previously developed method. Then a mode-matching technique is applied in order to obtain the reflection and transmission coefficients of the discontinuity. Numerical results are also given for several asymmetric step discontinuities.**

I. INTRODUCTION

Modelling of discontinuities in microstrip lines is highly important in analyzing the behavior of microwave and millimeter wave circuits.

A commonly encountered discontinuity structure in microstrip lines is the asymmetric abrupt change in strip line width, which can be employed in low pass filters, quarter-wavelength transformers and generally in a wide range of microwave circuits. In that sense it is very important to develop analytical techniques to treat this discontinuity problem, especially in high frequencies (above 10 GHz) where the lumped C and L description becomes less and less valid.

Microstrip discontinuity problems have been treated in the past by several authors [1]–[8]. Several comprehensive reviews on this matter are also presented in books [9]–[12]. The unshielded asymmetric microstrip step discontinuity is studied in [2], where a magnetic-wall model is employed. However, a full-wave analysis might be required in order to describe efficiently the discontinuity behavior at very high frequencies.

In this paper the concepts of the mode-matching techniques are employed in order to formulate a full-wave analysis of the boundary condition problem associated with the asymmetric microstrip step discontinuity. The fields on both sides of the discontinuity interface are expanded in terms of both even and odd hybrid modes. The characteristics of these modes are determined by using an analysis similar to [13] by Mittra and Itoh, which determined the dispersion characteristics of microstrip lines.

Then an efficient mode-matching procedure is developed by using products involving the orthogonal functions of both microstrip lines.

The technique used in this paper is similar to that developed previously by the authors [14] but now odd symmetry modes are taken into account in order to treat the asymmetric step microstrip discontinuities.

In the following analysis the time dependence of field quantities is assumed to be $\exp(j\omega t)$ and is suppressed throughout the analysis.

II. MODE CHARACTERISTICS OF THE MICROSTRIP

The geometry of the discontinuity problem under discussion is shown in Fig. 1. The step discontinuity is located at the $z = 0$ plane. The shielding box height and width are denoted by h and $2L$, respectively. Also the substrate dielectric constant and thickness are denoted by ϵ_r and d respectively

The conductive strip widths in the $z < 0$ and $z > 0$ regions are shown as $2t_1$ and $2t_2$ respectively, while ϵ denotes the axial displacement of the two microstrip lines on the $z = 0$ interface plane. Of course, the displacement of the two shielding boxes leads to an artificial geometry. However, it does not really affect the microstrip discontinuity itself, taking into account that this displacement is negligible compared to the shielding boxes' dimensions. Furthermore, a geometry where the shielding box is sufficiently wider than the microstrip is almost equivalent to the open microstrip asymmetric step discontinuity.

Because of the partial dielectric filling of the shielding box, only hybrid modes can be guided. The basic approach employed in the present analysis is the analytical technique developed by Mittra and Itoh [13] to determine the properties of both propagating and higher order evanescent modes. In [13] only even hybrid modes have been taken into account, while the asymmetric nature of the step discontinuity under study involves the properties of both odd and even modes. In the present analysis, the same notation as in [13], [14] is adopted.

In the odd mode case, the TM and TE field components are derived from the scalar potentials $\psi_i^{(e)}, \psi_i^{(h)}$ as follows:

$$
\begin{aligned}
\psi_1^{(e)} &= \sum_{n=1}^{\infty} A_n^{(e)} \sinh \cdot \alpha_n^{(1)} y \sin(\hat{k}_n x) \\
\psi_2^{(e)} &= \sum_{n=1}^{\infty} B_n^{(e)} \sinh \cdot \alpha_n^{(2)} (h-y) \sin(\hat{k}_n x) \\
\psi_1^{(h)} &= \sum_{n=1}^{\infty} A_n^{(h)} \cosh \cdot \alpha_n^{(1)} y \cos(\hat{k}_n x) \\
\psi_2^{(h)} &= \sum_{n=1}^{\infty} B_n^{(h)} \cosh \cdot \alpha_n^{(2)} (h-y) \cos(\hat{k}_n x)
\end{aligned} \tag{1}
$$

where the superscripts $(e), (h)$ are associated with E (TM) and H (TE) fields respectively, while the subscript $i = 1, 2$ designates the

Manuscript received March 12, 1991; revised June 15, 1992.
The authors are with the Department of Electrical Engineering, National Technical University of Athens, Athens 10682, Greece.
IEEE Log Number 9205465.

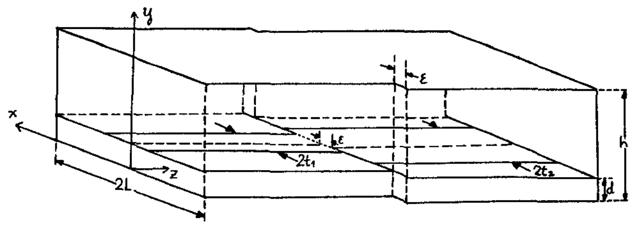

Fig. 1. Geometry of the discontinuity problem.

regions 1 ($0 < y < d$) and 2 ($d < y < h$). Also $\hat{k}_n = n\pi/L, \alpha_n^{(1)} = (\hat{k}_n^2 + \beta^2 - \epsilon_r k_o^2)^{1/2}, \alpha_n^{(2)} = (\hat{k}_n^2 + \beta^2 - k_o^2)^{1/2}$ and $k_o = \omega(\epsilon_o \mu_o)^{1/2}$ denotes the free-space wavenumber.

The scalar potentials $\psi_i^{(e)}$ and $\psi_i^{(h)}$ satisfy the two-dimensional Helmholtz equation and the boundary conditions on the side walls of the shielding box. In terms of these potential functions, the TE and TM fields can be expressed easily as described in [13], [14].

The computation of the characteristics of the even hybrid modes has been examined in [12], [14]. Following an analogous procedure, the odd hybrid mode characteristics can be determined by computing the nontrivial solutions of the same system as in [13], [14].

The mode propagation constants β and their associated mode expansion coefficients $\overline{A}_n^{(e)}, \overline{A}_n^{(h)}$ are computed numerically by truncating the infinite system into a finite order system, and this results in a highly converging procedure. The existence of complex modes is also taken into account [14], [15], [16].

Then the transversal field components $\underline{e}_m(x,y)$ and $\underline{h}_m(x,y)$ can be easily computed from (1) as

$$\underline{e}_m(x,y) = \nabla_t \cdot \psi_i^{(e)} - \frac{\omega\mu_o}{\beta_m}\hat{z} \times \nabla_t \psi_i^{(h)}$$
$$\underline{h}_m(x,y) = \frac{\omega\epsilon(y)}{\beta_m}\hat{z} \times \nabla_t \psi_i^{(e)} + \nabla_t \psi_i^{(h)} \tag{2}$$

where $i = 1\,(y < d)$ or $2\ (d < y < h)$, and m denotes the mode number.

Finally in the microstrip line the following mode power orthogonality relation is satisfied:

$$\iint_A \underline{e}_m(x,y) \times \underline{h}_{m'}^*(x,y) \cdot \hat{z}\, dx\, dy = \delta_{mm'} C_m \tag{3}$$

where (*) denotes the complex conjugate, A is the cross-sectional area of the microstrip, $\delta_{mm'}$ is the Kronecker delta, and the mode power coefficients C_m can be easily computed by an analogous procedure as for the even hybrid modes [14].

III. Mode-Matching Procedure

Consider an incident propagating wave ($\beta = \beta_1$) coming from $z = -\infty$ towards the $z = 0$ discontinuity plane. Then inside the $z < 0$ half-space the transversal electric and magnetic field components can be expressed as a superposition of the incident and the sum of all the even and odd reflected waves, while on the $z > 0$ half-space the transversal fields have the same structure without having the incident wave.

The trial of several approaches showed that there is an optimal strategy in terms of the convergence behavior as follows:

Taking vector products of the boundary conditions with the complex conjugate of the transversal field components and following the orthogonality properties of the $\underline{e}_r^{(x)}, \underline{h}_r^{(x)}, \underline{e}_r'^{(x)}$ and $h_r'^{(x)}$ eigenwaves, the following system of equations can be obtained:

$$(\delta_{1r}\delta^{(e)(x)}C_1^{(e)} - C_{1r}^{(e)(x)}) + \sum_{n=1}^{\infty} F_n^{(e)}(\delta_{nr}\delta^{(e)(x)}C_n^{(e)} - C_{nr}^{(e)(x)}) + \sum_{m=1}^{\infty} F_m^{(o)}(\delta_{mr}\delta^{(o)(x)}C_m^{(o)} - C_{mr}^{(o)(x)}) = 0 \tag{4}$$

$$C_{1r}^{(e)(x)} + \sum_{n=1}^{\infty} F_n^{(e)} C_{nr}^{(e)(x)} + \sum_{m=1}^{\infty} F_m^{(o)} C_{mr}^{(o)(x)} = \sum_{p=1}^{\infty} D_p^{(e)} C_{pr}^{(e)'(x)} + \sum_{q=1}^{\infty} D_q^{(o)} C_{qr}^{(o)'(x)} \tag{5}$$

$$C_{r1}^{*(x)'(e)} - \sum_{n=1}^{\infty} F_n^{(e)} C_{rn}^{*(x)'(e)} - \sum_{m=1}^{\infty} F_m^{(o)} C_{rm}^{*(x)'(o)} = \sum_{p=1}^{\infty} D_p^{(e)} C_{rp}^{*(x)'(e)'} + \sum_{q=1}^{\infty} D_q^{(o)} C_{rq}^{*(x)'(o)'} \tag{6}$$

$$\sum_{p=1}^{\infty} D_p^{(e)}(\delta_{pr}\delta^{(e)(x)}C_p^{(e)'} - C_{pr}^{(e)'(x)'}) + \sum_{q=1}^{\infty} D_q^{(o)}(\delta_{qr}\delta^{(o)(x)}C_q^{(o)'} - C_{qr}^{(o)'(x)'}) = 0 \tag{7}$$

where (x) can be either (e) or (o),

$$\delta^{(x)(y)} = \begin{cases} 1 & \text{when } (x) = (y) \\ 0 & \text{when } (x) \neq (y) \end{cases}$$

and $F_m^{(e)}, F_n^{(o)}, D_p^{(e)}$ and $D_q^{(o)}$ are unknown expansion coefficients to be determined.

$C_m^{(e)}$ and $C_m^{(o)}$ are defined in (3) and $C_{n1n2}^{(x1)(x2)}$ are coupling integrals defined as follows:

$$C_{n1n2}^{(x1)(x2)} = \int_0^h dy \int_{-L}^{L-\epsilon} dx\, (e_{n1}^{(x1)} \times h_{n2}^{*(x2)})\hat{z} \tag{8}$$

Finally ($'$) has been used to denote the space $z > 0$.

The system of (4)–(7) constitutes the basis of the analytical approach of this paper. The infinite summations are truncated into a finite order taking N terms (modes). Then convergence of the computed results is examined to verify the accuracy of the method.

The coupling integrals are computed by substituting the field expressions and then performing analytically the integrations with respect to x and y.

Then after computing the unknown coefficients $F_m^{(e),(o)}$ and $D_p^{(e),(o)}$, the reflection coefficient $S_{11} = F_1^{(e)}$ is obtained, while according to the definition of the S parameters the transmission coefficient S_{21} is obtained as follows.

$$S_{21} = D_1^{(e)} \left(\frac{C_1^{(e)'}}{C_1^{(e)}} \right)^{1/2} \tag{9}$$

Finally the power preservation theorem

$$|S_{11}|^2 + |S_{21}|^2 = 1 \tag{10}$$

is used in order to check the accuracy of the results.

TABLE I
CONVERGENCE SAMPLE OF THE PROPAGATION CONSTANT AND THE EXPANSION COEFFICIENT $A_n^{(e)}$

M	1	2	3	4	5	6	7
β mm⁻¹	-j0.842521	-j0.842528	-j0.842530	-j0.842531	-j0.842530	-j0.842529	-j0.842529
	-j3.055414	-j3.055355	-j3.055329	-j3.055326	-j3.055332	-j3.055339	-j3.055344
		-0.006108	-0.006145	-0.006149	-0.006141	-0.006132	-0.006124
			-0.003195	-0.003197	-0.003193	-0.003188	-0.003184
$A_n^{(e)}$				-0.001818	-0.001816	-0.001813	-0.001811
					-0.001029	-0.001026	-0.001025
						-0.000567	-0.000566
							-0.000301

f = 1 GHz, ϵ_r = 2.32, L = 4.7625 mm, h = 6.35 mm, t = 0.47625 mm.

TABLE II
NUMERICAL RESULTS FOR THE MODE PROPAGATION CONSTANTS AT 10 GHz

Frequency = 10 GHz		
2t₁ = 1.905 mm		
m	β(mm⁻¹) [even]	β(mm⁻¹) [odd]
0	0.2944+j0.0	-
1	0.0-j0.2478	0.0-j0.6230
2	0.0-j0.5540	0.0-j0.7963
3	0.0-j0.5935	0.0-j0.8154
4	0.0-j0.9652	0.0-j1.1697
2t₁ = 0.9525 mm		
m	β(mm⁻¹) [even]	β(mm⁻¹) [odd]
0	0.2883+j0.0	-
1	0.0-j0.2483	0.0-j0.6232
2	0.0-j0.5545	0.0-j0.7970
3	0.0-j0.5886	0.0-j0.8132
4	0.0-j0.9653	0.0-j1.1699

IV. NUMERICAL RESULTS

Numerical computations have been performed by applying the theory presented above. For each pair of microstrip lines the spectrum and the unknown modal expansion coefficients of both even and odd propagating and evanescent waves are determined up to sufficient order by taking $2M$ equations in the system used in [13]. Then the system of (4)–(7) is solved numerically by keeping N terms in the infinite summations. Extensive convergence tests have been performed in order to verify the accuracy of the obtained scattering parameters in conjunction to M and N truncations; a sample is presented in Table I. The numerical stability and the satisfaction of the power conservation theorem were verified in each case. Furthermore the convergence to the symmetric step discontinuity was verified in the case where the eccentricity tends to zero [14].

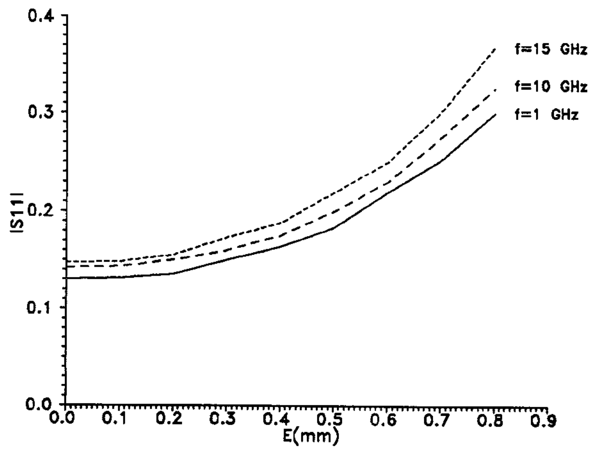

Fig. 2. Variation of $|S_{11}|$ with respect to the eccentricity.

In the computed results the shielding box dimensions are taken to be

$$2L = 9.53\,\text{mm}, \quad h = 6.35\,\text{mm}.$$

The substrate height is $d = 0.635$ mm and the dielectric constant is $\epsilon_r = 2.32$. The two microstrip line widths are

$$2t_1 = 0.9525\,\text{mm}, \quad 2t_2 = 1.905\,\text{mm}.$$

In Table II the spectrum of both even and odd hybrid modes is presented for the two microstrip lines at a frequency of 10 GHz. The odd evanescent modes have exactly the same capacitive or inductive behavior as the corresponding even ones (i.e. first odd compares to first even, etc.). In Figs. 2 and 3 the variation of the S_{11} and S_{21} parameters is presented with respect to the eccentricity ϵ at 1 GHz,

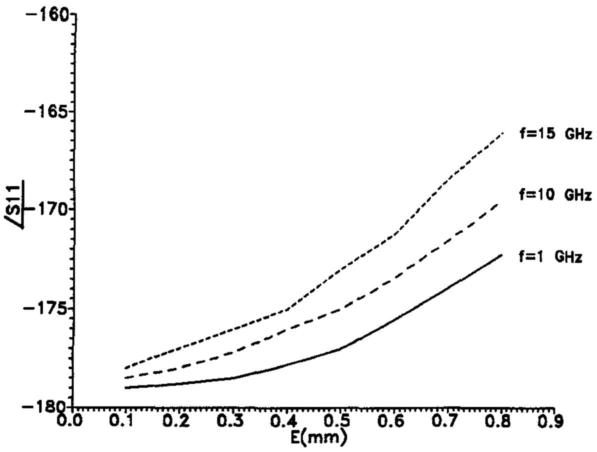

Fig. 3. Variation of $\angle S_{11}$ with respect to the eccentricity.

10 GHz and 15 GHz. Notice that strong reflections are observed as the eccentricity becomes comparable to the microstrip line widths.

V. Conclusions

A frequency-dependent analysis of the shielded microstrip asymmetric step discontinuity has been presented. The asymmetric nature of the discontinuity requires the investigation of the spectrum of both odd and even hybrid modes. Numerical results have been presented and the effect of the eccentricity on the scattering parameters has been depicted. In principal the same method can be employed to treat other types of asymmetric discontinuity problems.

References

[1] N. H. L. Koster and R. H. Jansen, "The microstrip step discontinuity: a revised description," *IEEE Trans. Microwave Theory Tech.*, vol. MTT-34, pp. 213–222, 1986.

[2] T. Chu and T. Itoh, "Generalized scattering matrix method for analysis of cascaded and offset microstrip step discontinuities," *IEEE Trans. Microwave Theory Tech.*, vol. MTT-34, pp. 280–284, Feb. 1986.

[3] Benedek and P. Sylvester, "Equivalent capacitances for microstrip gaps and steps," *IEEE Trans. Microwave Theory Tech.*, vol. MTT-20, pp. 729–733, 1972.

[4] A. F. Thomson and A. Gopinath, "Calculation of microstrip discontinuity inductances," *IEEE Trans. Microwave Theory Tech.*, vol. MTT-23, pp. 177–179, 1972.

[5] G. Kompa, "Design of stepped microstrip components," *Radio Electron. Eng.*, vol. 48, pp. 53–63, 1978.

[6] R. H. Jansen, "The spectral domain approach for microwave integrated circuits," *IEEE Trans. Microwave Theory Tech.*, vol. MTT-33, pp. 1043–1056, 1985.

[7] T. S. Chu, T. Itoh, and Yi Chi Shih, "Comparative study of mode matching formulations for microstrip discontinuity problems," *IEEE Trans. Microwave Theory Tech.*, vol. MTT-33, pp. 1018–1023, 1985.

[8] R. K. Hoffman, *Integrierte Mikrowellenshcaltungen.* Berlin: Springer-Verlag, 1983.

[9] K. C. Gupta, R. Garg, and I. J. Bahl, *Microstrip Lines and Slotlines.* Dedham, MA: Artech House, 1979 sec. 3.4.3.

[10] K. C. Gupta, R. Garg, and R. Chadha, *Computer Aided Design of Microwave Circuits.* Dedham, MA: Artech House, 1981 sec. 6.2.4.

[11] T. C. Edwards, *Foundations for Microstrip Circuit Design.* ch. 5, New York: Wiley, 1981.

[12] R. Mehran, *Grundelemente des rechnergestutzen Entwurfs von Mikrostreifenleitungs-Schaltungen.* Aachen: Verlag. H. Wolff, 1983.

[13] R. Mittra and T. Itoh, "A new technique for the analysis of the dispersion characteristics of microstrip lines," *IEEE Trans. Microwave Theory Tech.*, vol. MTT-19, pp. 47–56, 1971.

[14] N. Uzunoglu, C. Capsalis, and C. Chronopoulos, "Frequency dependent analysis of a shielded microstrip step discontinuity using an efficient mode-matching technique," *IEEE Trans. Microwave Theory Tech.*, vol. 36, pp. 976–984, 1988.

[15] J.-T. Kuo and C.-K. C. Tzang, "Complex modes in shielded suspended coupled microstrip lines," *IEEE Trans. Microwave Theory Tech.*, vol. 38, pp. 1278–1286, Sept. 1990.

[16] S. Omar and K. Schuenemann, "The effect of complex modes at finline discontinuities," *IEEE Trans. Microwave Theory Tech.*, vol. MTT-34, pp. 1508–1514, Dec. 1986.

Semi-Discrete Finite Element Analysis of Zero-Thickness Inductive Strips in a Rectangular Waveguide

Devin Crawford and Marat Davidovitz

***Abstract*—A semi-discrete finite element method is applied to determine the network parameters for zero-thickness inductive discontinuities in a rectangular guide. The solution obtained is computationally efficient and is applicable under multi-mode conditions. Moreover, after obtaining the solution for a given geometry at a specific frequency, further frequency analysis for the same geometry requires only nominal additional recalculation. Convergence properties of the solution are studied and comparison with published data is carried out to verify the solution accuracy.**

I. Introduction

A variant of the FEM, the Semi-Discrete Finite Element Method (SDFEM) utilizes the properties of the FEM in one plane of the domain, while the solution along the remaining dimension is found analytically. Thus, the computational burden associated with this method is considerably smaller than that for a fully-discrete FEM solution. Moreover, in the framework of the SDFEM, radiation condition can be rigorously applied along certain directions in a Cartesian coordinate system. Therefore, the SDFEM is suited to problems involving discontinuities in a plane. Here we examine the problem of zero-thickness inductive discontinuities in a waveguide. This problem has been extensively studied in the past [1], [2], [3], [4], [7], and therefore is a good model problem with which to verify the proposed method, as well as examine its characteristics in detail.

Section II of this paper deals with the theoretical formulation of the problem, based on the scalar Helmholtz equation for the TE field. In Section III the numerical issues of discretization, convergence and execution time are examined. In section IV, we compare our results with published data [7] and finally, Section V contains conclusions and suggestions for further work.

II. Formulation of the Problem

Consider a general, infinitesimally thin inductive diaphragm shown in Fig. 1. It is assumed that the TE_{10} mode is incident from $z < 0$. It is well-known [5] that for this type of discontinuity only higher-order TE_{n0} modes are excited. Therefore the scattered TE field satisfies the

Manuscript received February 4, 1992; revised June 30, 1992.
The authors are with the Department of Electrical Engineering, University of Minnesota, 200 Union Street SE, Minneapolis, MN 55455.
IEEE Log Number 9205466.

0018–9480/93$03.00